

We are IntechOpen, the world's leading publisher of Open Access books Built by scientists, for scientists

6,900

Open access books available

185,000

International authors and editors

200M

Downloads

Our authors are among the

154

Countries delivered to

TOP 1%

most cited scientists

12.2%

Contributors from top 500 universities



WEB OF SCIENCE™

Selection of our books indexed in the Book Citation Index
in Web of Science™ Core Collection (BKCI)

Interested in publishing with us?
Contact book.department@intechopen.com

Numbers displayed above are based on latest data collected.
For more information visit www.intechopen.com



On Thermal Conductivity of an In-Situ Metal Matrix Composite - Cast Iron

J.K.Chen and S.F.Chen

*National Taipei University of Technology/ Inst. Materials Science and Engineering
Taiwan, R.O.C.*

1. Introduction

Cast iron is a typical in-situ metal matrix composite consisting of graphite, ferrite, and pearlite microstructures. It is well known that a great range of strength and ductility can be attained by controlling the shapes of graphite and alloy design in cast irons. With increasing applications of cast irons in high temperature environment, e.g. disc brakes, engine exhaust manifolds and cylinders, etc., thermal conduction properties of such materials are particularly important.

Modelling of thermal conductivity for composite, however, is not an easy materials property to deal with especially for a heterogeneous material such as cast iron. The cast irons represent a combination of graphite with different shapes, ferrite, and pearlite. Furthermore, alloying elements can affect their thermal conductivity in two aspects: the inherent thermal conductivity of various phases and the stability of different phases due to compositional changes (Helsing and Grimvall 1991).

The current article treats cast iron as a metal matrix composite via application of effective-medium theories. The effects of three factors upon thermal conductivity of cast irons are discussed including matrix phases, shapes of graphite, and alloying elements. These effects are concerned with the anisotropic properties and morphology of second phase particles in composites. For example, pearlite stands for lamellar composite structure, whereas nodular and flake graphite represents different shapes of second phase particles. It is thus the objective of this article to discuss the effects of different phases and their morphology on thermal conductivity of cast irons through both measurement and theoretical predictions.

The study starts out with the review of theorems describing thermal conductivity of composites. Effective Medium Theory is of particular interest for applications in cast irons for its versatility in modeling different second phase particle morphology and lamellar structures. Both room temperature and high temperature thermal conductivity of cast irons and basic matrix structures are measured to compare with theoretically predicted values. Furthermore, nodular, compact, and flake graphite are formed by alloying and casting process controls.

Thermal conductivities of cast irons range widely from 20 to 70 W/m/°C. It is found that the calculated thermal conductivity matches well with the measured values. The grey irons with flake graphite greatly increase thermal conductivity due to its anisotropy. Nodular irons then have lower thermal conductivity. Ferrite structure has nearly twice the thermal conductivity of lamellar pearlitic matrix. Alloying elements then have two-fold effects on thermal conductivity of cast irons, one on the intrinsic thermal conductivity of different

microstructures and the other on amount of constituent phases. It is observed that effects of alloying elements to thermal conductivity fall mainly on the amount of different phases formed rather than on phase compositions. The current work demonstrates an integrated path for thermal conductivity modelling in complex composite systems.

2. Theory

Concepts of effective medium theory or effective medium approximations were originated from the work by Maxwell-Garnett (1904) and Bruggeman (1935). Many extended formulas have since been developed with these bases (Choy, 1999). Such approximation was developed to describe the physical properties of heterogeneous bodies through combination of homogeneous isotropic phases. The combined composites thus give rise to an effective property corresponding to a homogeneous medium. As the development of effective medium theory was based upon the effects of polarization under influence of electromagnetic fields, the most common physical properties considered using effective medium theory are conductivity and dielectric constants among all.

In Cheng and Vachon's (1969) study, thermal conductivity of two and three phase solid heterogeneous mixtures were considered based upon Tsao's (1961) model. Tsao's model slices the composite bodies into parallel plates in perpendicular to heat transfer direction. Fractions of discontinuous phases in each plate attribute to the solutions of an effective quantity. The effective quantity such derived thus is inappropriate for describing the anisotropic phase such as graphite flakes in cast irons.

The methodology developed by Helsing and Helte (1991) is of interest in current article which treats a continuous medium as an isotropic aggregate of anisotropic grains. The concept was based upon Schulgasser's (1977) study on the conductivity of polycrystalline materials whereas each equiaxial crystals are aligned in varied orientation (Fig.1). Such model is especially advantageous in constructing ferritic and pearlitic matrix structures in cast irons. The anisotropic nature of graphite and pearlitic grains can thus be simulated.

2.1 Thermal conductivity of matrix phase

2.1.1 Thermal conductivity of ferritic matrix

For a ferritic matrix of varied compositions, it is necessary to consider both its phonon and electronic thermal conductivity. The electronic thermal conductivity can be derived using Lorenze function, L_e , relating the electronic thermal conductivity, K_e , and electrical resistivity, ρ_m , of pure iron by Wiedemann-Franz law:

$$K_{e,\text{pure iron}} = \left(\frac{\rho_m}{L_e T} \right)^{-1} \quad (1)$$

For ferritic alloys, the effects of alloying alloying elements must also be added by considering the electrical resistivity of i th element (Williams, 1981):

$$K_{e,\text{ferrite}} = \left(\frac{\rho_m}{L_e T} + \frac{1}{L_o T} \sum_i \rho_i' C_i \right)^{-1} \quad (2)$$

where L_o is the Sommerfeld-Lorenz number of $2.44 \times 10^{-8} \text{ W}\Omega^\circ\text{C}^{-2}$, ρ_i' is relative electrical resistivity of i -th alloying element in comparison with pure iron, C_i is the concentration of i -

th element in molar fraction, and T is temperature. The L_e term represents the changes of Lorenz function of pure iron with temperature and is assumed to be independent of alloying elements (Table 1.) Therefore, Eqn.(2) comprises of temperature-dependent part of electrical thermal conductivity for pure iron and the second term considering variations caused by alloying elements.

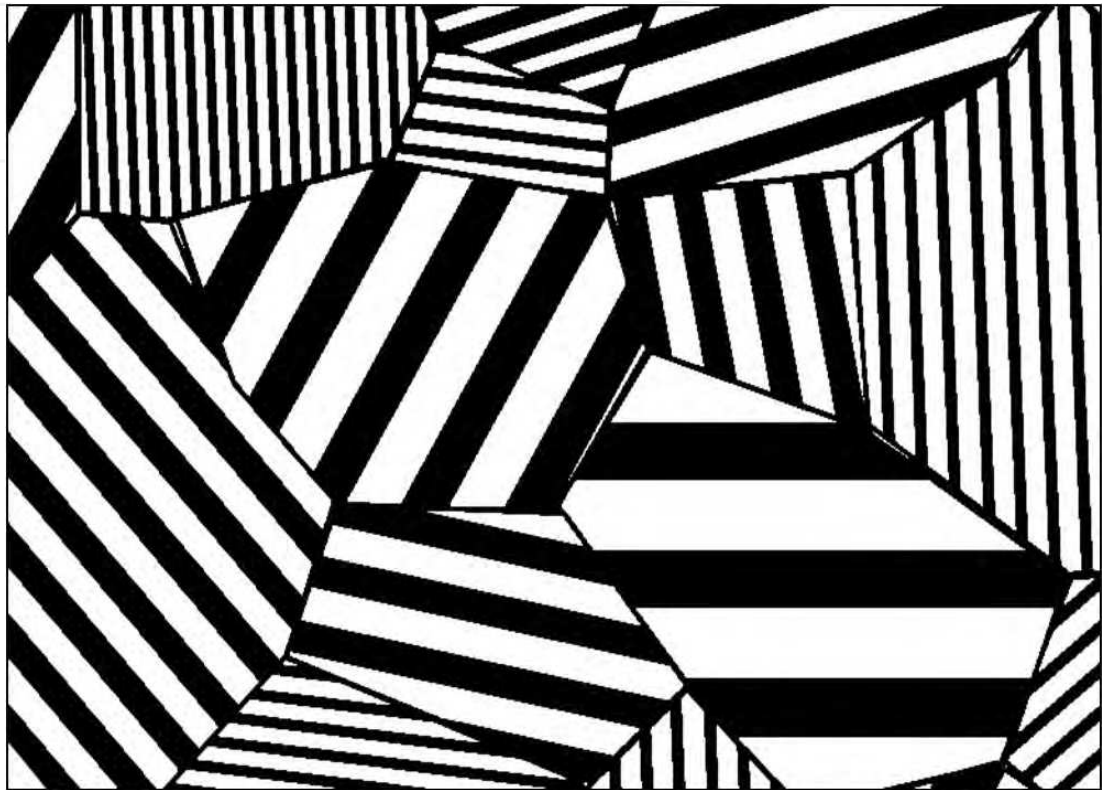


Fig. 1. Schematics of polycrystals with anisotropic grains (from Schulgasser 1977)

	27°C	100°C	200°C	300°C
ρ_m $\mu\Omega\text{ cm}$	11.16	14.76	21.76	27.36
$L_e \times 10^8$ $W\Omega^\circ C^{-2}$	2.03	2.09	2.22	2.31

Table 1. Lorenz functions and resistivity of pure iron at different temperature (Williams, 1981)

The contribution of lattice vibration to thermal conductivity in ferrite, $K_{p,ferrite}$, is then expressed by

$$K_{p,ferrite} = (\frac{1}{K_{p,pure\ iron}} + \sum_i A_i C_i)^{-1} \tag{3}$$

where $K_{p,pure\ iron}$ is the phonon contribution of thermal conductivity in pure iron, and the second term in Eqn.(3) represents the phonon scattering (A_i) due to impurity atoms, i .

	Si	Al	Cr	Mo
ρ_i' $\mu\Omega\text{ cm/at.}\%$	7	6.4	4.6	4.8
$10^3\times A_i$ $\text{m}^\circ\text{C/W/at.}\%$	8	7	0.1	13

Table 2. Coefficients ρ_i' and A_i (Helsing and Grimvall, 1991) for different alloying elements

Therefore, the thermal conductivity of ferrite, K_{ferrite} , is simply the combination of electrical and phonon contributions,

$$K_{\text{ferrite}}=K_{\text{e,ferrite}}+K_{\text{p,ferrite}} \tag{4}$$

2.1.2 Thermal conductivity of pearlitic matrix

Pearlite structure is represented by ferrite and cementite in parallel lamellae. Apparently, such structure is anisotropic, while the aggregation of anisotropic grain should give rise to an effective thermal conductivity. Thermal conductivity of pearlite parallel to the lamellae can be written as

$$K_{\text{pearlite,//}}=f_{\text{Fe}_3\text{C}}\ K_{\text{Fe}_3\text{C}}+f_{\text{ferrite}}\ K_{\text{ferrite}} \tag{5}$$

and that of pearlite perpendicular to the lamellae is

$$K_{\text{pearlite,\perp}}=(f_{\text{Fe}_3\text{C}}\ /K_{\text{Fe}_3\text{C}}+f_{\text{ferrite}}\ /K_{\text{ferrite}})^{-1} \tag{6}$$

where $f_{\text{Fe}_3\text{C}}$ (=0.122) and f_{ferrite} (=0.878) are the volume fractions of Fe_3C and ferrite, respectively. $K_{\text{Fe}_3\text{C}}$ is the thermal conductivity of cementite or 8 W/m/°C (Helsing and Grimvall, 1991). The effective isotropic thermal conductivity of pearlite, $K_{\text{pearlite}}^{\text{eff}}$, estimated by Effective medium approximation is thus given by (Helsing and Grimvall, 1991)

$$K_{\text{pearlite}}^{\text{eff}}=\frac{1}{4}[K_{\text{pearlite,//}}+\sqrt{K_{\text{pearlite,//}}^2+8K_{\text{pearlite,//}}K_{\text{pearlite,\perp}}}] \tag{7}$$

The $K_{\text{pearlite,//}}$ is calculated to be in the order of 58W/m/°C, whereas $K_{\text{pearlite,\perp}}$ is only around 35W/m/°C. The effective thermal conductivity of pearlite is thus in the order of 45~50W/m/°C.

2.1.3 Experimental and theoretical thermal conductivity of matrix

Thermal conductivities of bulk matrix materials are measured using interstitial free steel (C<50ppm) and AISI 1080 (C=0.80wt%) steels to simulate ferrite and pearlite structure. Fig. 2 shows the microstructures of these samples.

Thermal conductivities of ferrite and pearlite materials are measured by hot disk method (Gustafsson, 1991) using two specimens with size of 50mm dia × 20mm t. The predicted values by combining Eqns. (1)~(7) are shown to bear good agreement with the measured values as shown in Fig. 3.

It is observed that there is a great difference in thermal conductivity of ferritic and pearlitic matrices. This does not necessarily all arise from the contribution of cementite which

account for about 6.9W/m/°C of difference only. The main reduction of thermal conductivity is due to the stacking of ferrite and cementite. The conductivity in orientation perpendicular to the pearlitic lamellae, $K_{pearlite,\perp}$ is only 60% of conductivity in orientation parallel to the pearlitic lamellae indicating that the lamellar structures stand for a regular and great barrier for both electron and phonon conduction.

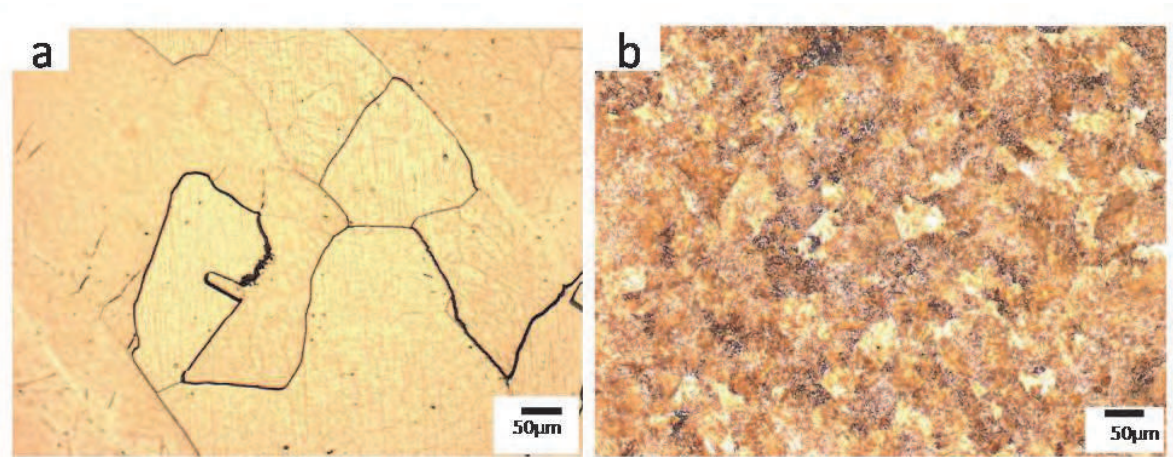


Fig. 2. Microstructures of (a) ferrite and (b) pearlite structures

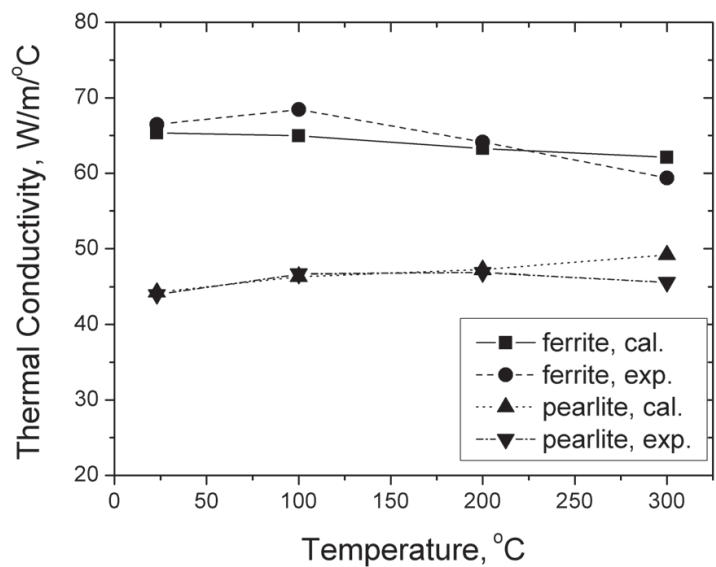


Fig. 3. Calculated (cal.) and measured (exp.) thermal conductivity of ferrite and pearlite structures.

2.2 Effects of graphite types on thermal conductivity

2.2.1 Thermal conductivities of cast irons with different graphite morphology

Different types of graphite affect the mechanical properties of cast irons greatly. There are two extreme shapes of graphite, namely spherical and flake graphite. In the current study, besides the ductile irons (FCD) with spherical graphite and the conventional grey irons (FC) with flake graphite, cast irons with compact graphite (CGI) that fall in between the two extreme cases is also considered.

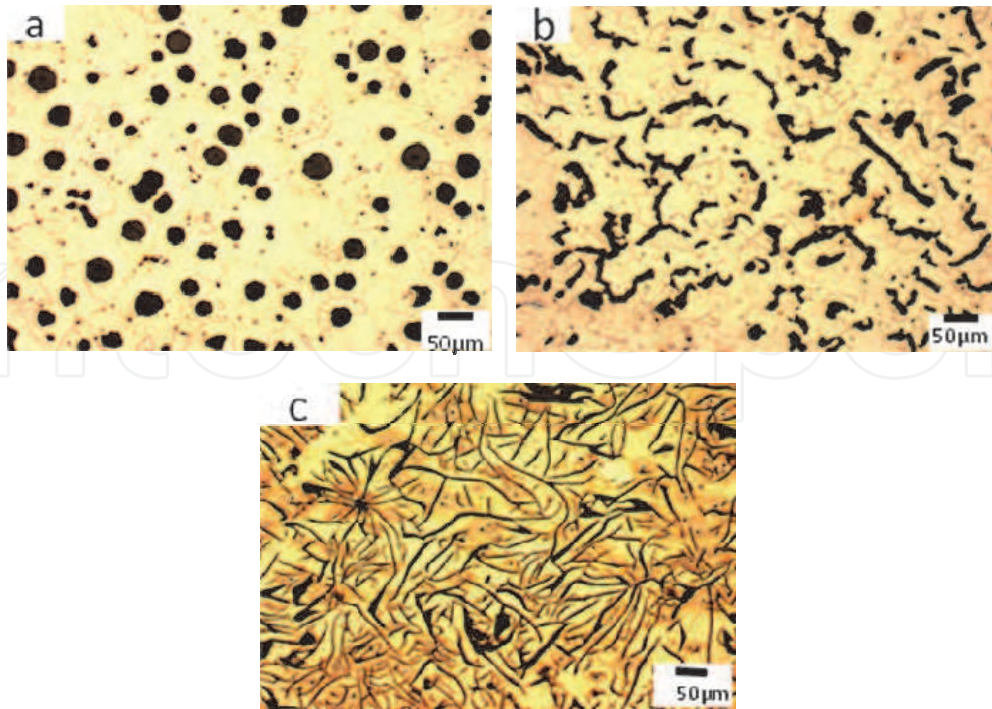


Fig. 4. OM microstructures of (a) nodular iron (FCD), (b) compact graphite iron (CGI), and (c) grey iron (FC) specimens

The FC specimen is a JIS FC250 grade cast iron with carbon equivalence of 3.83. The FCD sample is prepared using a JIS FCD450 grade iron (CE%=4.51) spheroidized using 1.1wt% of spheroidizer for 40s prior casting. And the CGI sample is then prepared by the same FCD450 grade iron spheroidized using 0.5wt% spheroidizer for 60s to deteriorate the nodular graphite formation.

From the microstructures shown in Fig. 4, it is apparent that the grey irons (Fig. 4c) with flake graphite give rise to highly anisotropic properties due to its characteristic planar shapes. The conductivity in orientations parallel to the flake surface is far higher than that in perpendicular direction. The effective thermal conductivity of grey iron is obtained by solving the following equation:

$$K_{\text{cast iron}}^{\text{eff}} = K_{\text{matrix}} + 3f_{\text{other}} K_{\text{cast iron}}^{\text{eff}} \left(\frac{K_{\text{other}} - K_{\text{matrix}}}{2K_{\text{cast iron}}^{\text{eff}} + K_{\text{o}}} \right) + \frac{1}{3} f_{\text{graphite}} K_{\text{cast iron}}^{\text{eff}} \left[\frac{K_{\text{graphite},\perp} - K_{\text{matrix}}}{K_{\text{cast iron}}^{\text{eff}} + p_{\perp} (K_{\text{graphite},\perp} - K_{\text{cast iron}}^{\text{eff}})} + 2 \frac{K_{\text{graphite},//} - K_{\text{matrix}}}{K_{\text{cast iron}}^{\text{eff}} + p_{//} (K_{\text{graphite},//} - K_{\text{cast iron}}^{\text{eff}})} \right] \quad (8)$$

Here the shape factors in orientation parallel and perpendicular to graphite flakes, $p_{//}$ and p_{\perp} , are written as

$$p_{//} = \varepsilon(2 - 2\varepsilon^2)^{-1} [(1 - \varepsilon^2)^{-\frac{1}{2}} \cos^{-1}(\varepsilon) - \varepsilon] \quad (9)$$

$$p_{\perp} = 1 - 2p_{//} \quad (10)$$

, respectively. The ε parameter represents the thickness-length ratio of graphite and is assumed to be 0.05 for FC specimens. The thermal conductivities of graphite in direction parallel and perpendicular to flake surface, $K_{\text{graphite},//}$ and $K_{\text{graphite},\perp}$, are taken to be 500 and 10 W/m/°C, respectively (Helsing and Grimvall, 1991).

For ductile cast irons with spherical graphite shape, thermal conductivity can be solved by the following:

$$K_{\text{ductile iron}}^{\text{eff}} = K_{\text{matrix}} + 3f_{\text{other}} K_{\text{cast iron}}^{\text{eff}} \left(\frac{K_{\text{other}} - K_{\text{matrix}}}{2K_{\text{cast iron}}^{\text{eff}} + K_{\text{o}}} \right) + f_{\text{graphite}} \left(\frac{3}{2 + \eta K_{\text{graphite},\perp} / K_{\text{ductile iron}}^{\text{eff}}} \right) \left(\frac{2K_{\text{graphite},//} + \eta K_{\text{graphite},\perp}}{2 + \eta} - K_{\text{matrix}} \right) \quad (11)$$

where f_{other} and K_{other} are the volume fraction and thermal conductivity of other microconstituents such as austenite or carbides, and

$$\eta = \frac{1}{2} \left[\left(1 + \frac{8K_{\text{graphite},//}}{K_{\text{graphite},\perp}} \right)^{\frac{1}{2}} - 1 \right] \quad (12)$$

As for CGI specimens that have graphite morphology in between nodular and flake shape, an equation by combining Eqns. (8) and (11) linearly can be derived. Fractions of graphite with nodular shape and flake shape, $f_{\text{nodular graphite}}$ and $f_{\text{flake graphite}}$, are taken into account by the following equation:

$$K_{\text{ductile iron}}^{\text{eff}} = K_{\text{matrix}} + 3f_{\text{other}} K_{\text{cast iron}}^{\text{eff}} \left(\frac{K_{\text{other}} - K_{\text{matrix}}}{2K_{\text{cast iron}}^{\text{eff}} + K_{\text{o}}} \right) + \frac{1}{3} f_{\text{flake graphite}} K_{\text{cast iron}}^{\text{eff}} \left[\frac{K_{\text{graphite},\perp} - K_{\text{matrix}}}{K_{\text{cast iron}}^{\text{eff}} + p_{\perp} (K_{\text{graphite},\perp} - K_{\text{cast iron}}^{\text{eff}})} + 2 \frac{K_{\text{graphite},//} - K_{\text{matrix}}}{K_{\text{cast iron}}^{\text{eff}} + p_{//} (K_{\text{graphite},//} - K_{\text{cast iron}}^{\text{eff}})} \right] + f_{\text{nodular graphite}} \left(\frac{3}{2 + \eta K_{\text{graphite},//} / K_{\text{ductile iron}}^{\text{eff}}} \right) \left(\frac{2K_{\text{graphite},\perp} + \eta K_{\text{graphite},//}}{2 + \eta} - K_{\text{matrix}} \right) \quad (13)$$

2.2.2 Calculated and measured thermal conductivity for cast irons with different graphite morphology

Fig. 5. demonstrates the calculated and measured thermal conductivity for different cast irons in Fig. 4. The compact graphite and grey iron samples show good agreement between the calculated and experimental values at temperatures below 100°C but diverge at temperatures over 200°C. Further observations note that the measured thermal conductivities are consistently lower with increasing temperatures. This is due to that the temperature dependence of graphite conductivity is not considered. Therefore, an estimated -3000ppm/°C of temperature coefficient of thermal conductivity for graphite is employed in Fig. 6. The predicted thermal conductivities apparently improve consistency with the measured values when temperature dependence of graphite thermal conductivity is considered.

It is also observed that the grey irons have the highest conductivity among all in comparison with nodular irons and compact graphite irons. The difference can be as large as 2~3 times.

This suggests that the anisotropic properties of grey irons improve their effective conductivity. It is attributed to the aligned graphite flake in random orientations to increase overall thermal conduction activities. Even though the compact graphite irons consist of graphite similar in shape with grey irons, their effective thermal conductivities are closer to those of nodular irons.

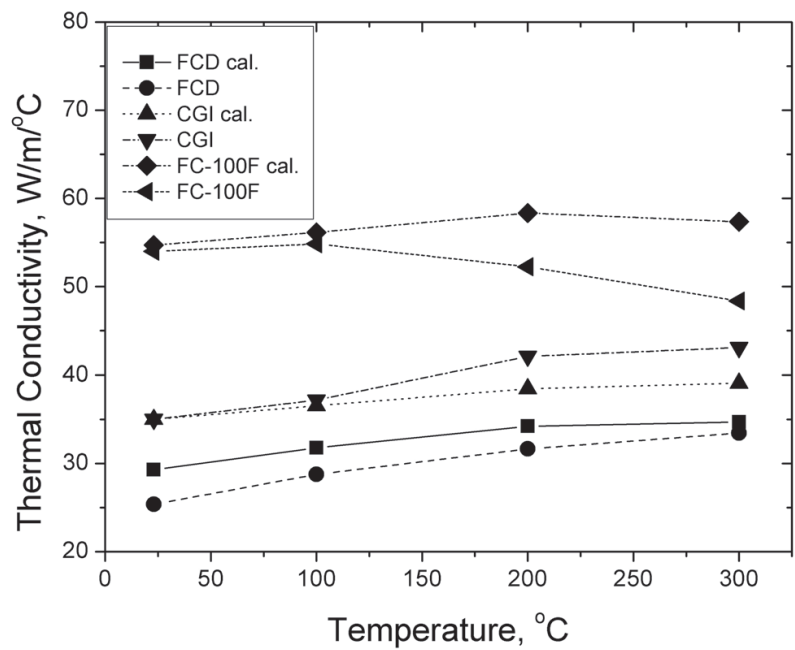


Fig. 5. Calculated (cal.) and measured thermal conductivity of grey irons (FC), compact graphite irons (CGI), and nodular irons (FCD).

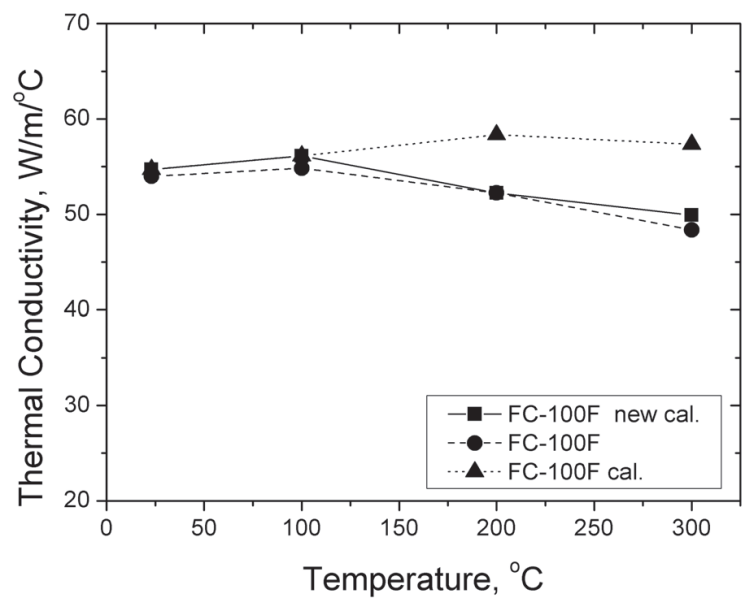


Fig. 6. Thermal conductivities of grey irons considering temperature dependence in thermal conductivity of graphite (new cal.) in comparison with non-temperature dependence predicted values (cal.) and measured values.

2.3 Effects of alloying elements on thermal conductivity

The alloying elements have two effects on thermal conductivity of cast irons. Different alloying elements can affect constituents of microstructures. Alloying elements such as Si and Cu are graphite stabilizer, while Cu also promotes pearlite formation (Figs.7a and 7b). On the other hand, Mo and Cr are carbide stabilizers. Therefore, different alloying elements induce different amount of graphite and matrix types (Fig. 7.)

Fig.6. demonstrates a series of FC samples with 1 additional wt.% of Si, Cu, Cr, Mo, and Al. For example, in Fig. 7b, the grey iron with 1wt.% of Cu addition indeed promote the matrix to form pearlite while graphite flakes appear to be thinner and smaller in comparison with the iron with 1wt.% Si addition in Fig. 7a.

For Cr and Mo added grey irons, the matrix apparently gives rise to many white areas which correspond to alloy carbides and would need to be taken into account in consideration of thermal conductivity. On the other hand, the 1wt.% aluminium added grey iron bear great amount of ferrite adjacent to the graphite. Alloying elements control the amount of different microconstituents formed and affect the thermal conductivities of alloyed grey irons.

Meanwhile, the alloying elements can also affect the compositions of different microstructures, such as ferrite and carbides. It is observed that the morphology of graphite varies with elements added. These will affect the values estimated by Eqn.(2) and thus demonstrate the dependence of thermal conductivity on alloying elements.

In considering the thermal conductivity of cast irons with alloying elements, quantitative metallography and SEM-EDS analyses are utilized to calculate the amount of different phases and to confirm the compositions of each microconstituent. Compositions of each constituent phase can thus be entered into the equations to estimate the thermal conductivity of each phase.

Fig. 8 demonstrates the dependence of thermal conductivity with alloying elements. In Fig.6, the base thermal conductivity of FC grey iron is $\sim 55\text{W/m/}^\circ\text{C}$ at room temperature. This value is compared with those measured or predicted in alloyed irons in Fig. 8. It is observed that all alloying elements pose a reduction effect on thermal conductivity. This is attributed to the scattering of both electrons and phonons by the impurity atoms in grey irons.

Among all alloying elements added, aluminum and copper has the least effects on reduction of thermal conductivity. In Table 2, it is noted that aluminum does not necessarily give a higher electrical resistivity and phonon scattering effects in comparison with other alloying elements. The lesser reduction effects on thermal conductivity are mostly likely from the microstructure factor. In particular, graphite stabilizer, such as copper and aluminum, can generate higher number of thinner graphite which compensates some negative effects of alloying elements upon thermal conductivity.

The carbide formers, chromium and molybdenum, have two-fold effects on the thermal conductivity. They not only affect the overall thermal conductivity by carbide formation but also reduce the graphite formation. Chromium has a relatively smaller effect on phonon scattering (Table 2) and shows a little higher conductivity value than molybdenum alloyed irons. Molybdenum gives the highest phonon scattering effects among the alloying elements and gives rise to the lowest thermal conductivity in Fig. 8.

In summary, reduction of thermal conductivity in cast irons is mostly attributed to the microstructures affected by the alloying elements. Amount of flake graphite, carbide, and ferrite can all contribute to the combined thermal conductivity. The composition in each phase, such as ferrite, affects less pronounced on the effective conductivity.

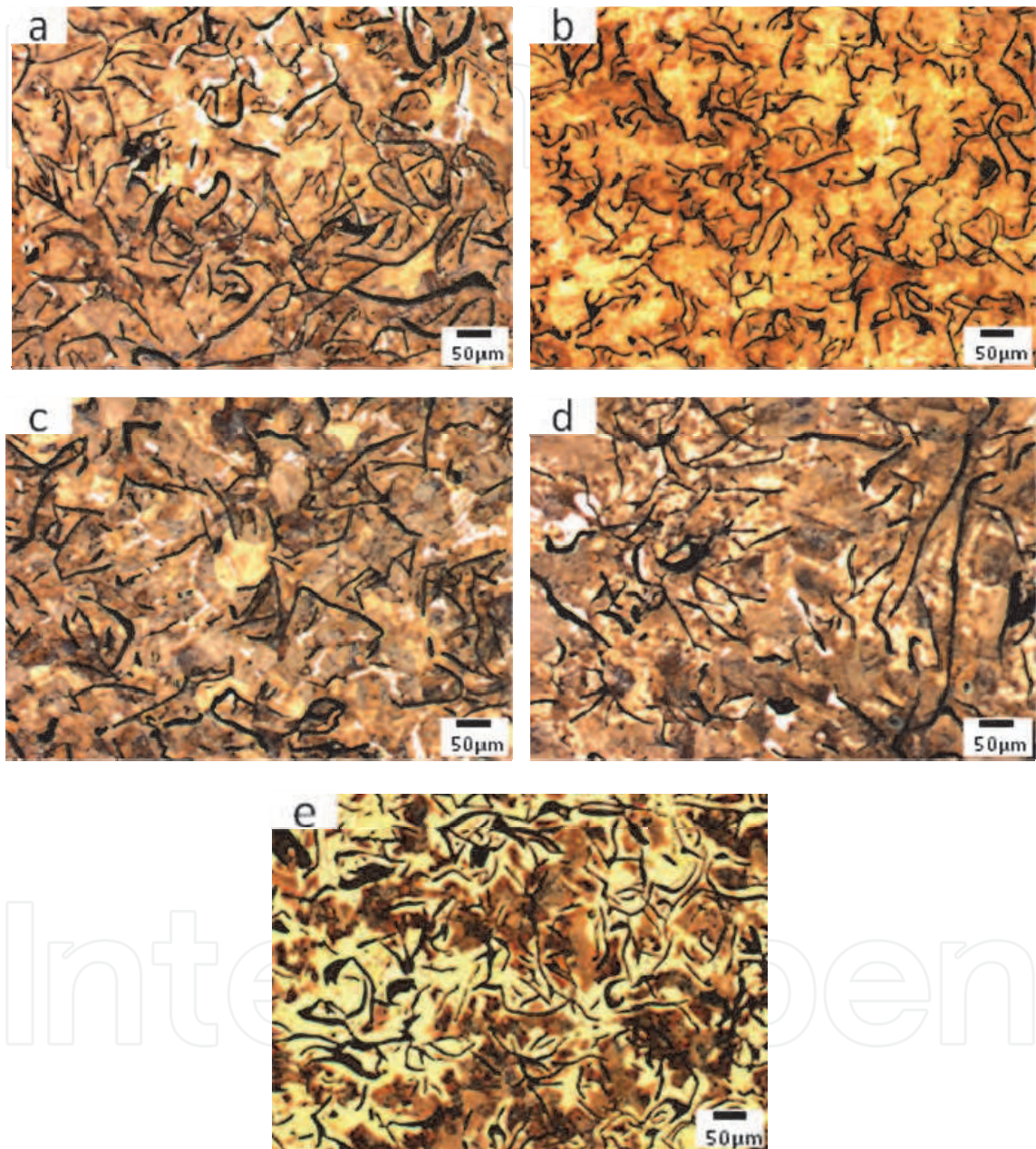


Fig. 7. Optical microstructures of (a) FC-1wt.%Si, (b) FC-1wt.%Cu, (c) FC-1wt.%Cr, (d) FC-1wt.%Mo, and (e) FC-1 wt.%Al specimens.

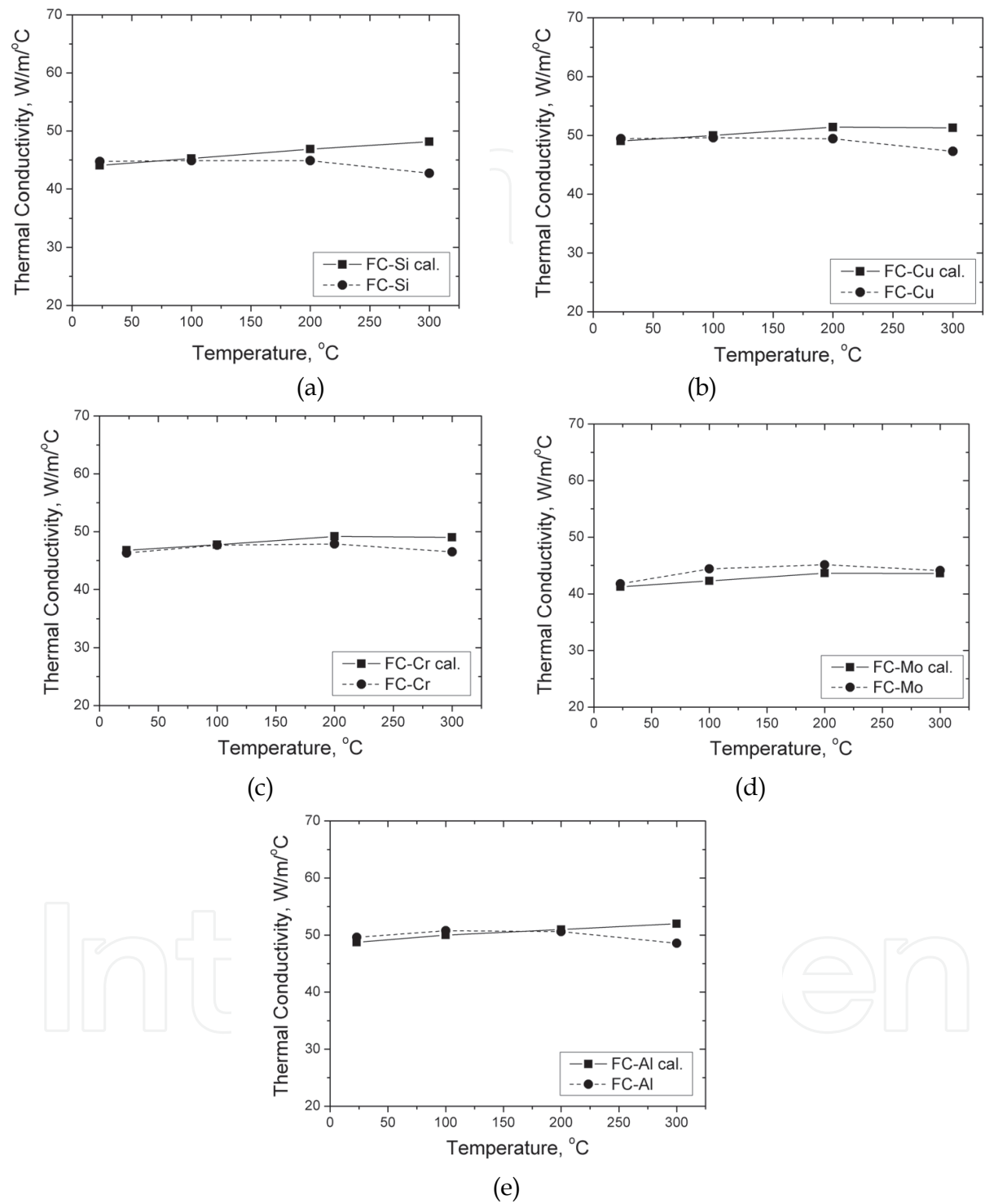


Fig. 8. Measured thermal conductivities of (a)FC-1 wt.%Si, (b)FC-1 wt.%Cu, (c)FC-1 wt.%Cr, (d)FC-1 wt.%Mo, and (e)FC-1 wt.%Al specimens and their predictions (cal.)

3. Conclusion

Current study reports the effects of microstructures, alloying elements, and graphite morphology on thermal conductivity of cast irons through both experimental measurements and theoretical estimations. Good agreement can be found in between the measured and estimated values using effective medium approximations. Reasons for great differences of thermal conductivity among cast irons of different types can thus be discussed. The following conclusions are drawn from these discussions.

1. Ferrite structure has as large as an order of magnitude of thermal conductivity higher than that of cementite. When the two structures are stacked in layers, the anisotropic properties cause the orientations in parallel and in perpendicular to the lamellae structure to have a 60% difference. This greatly affects the effective thermal conductivity of pearlite indicating that the interfaces between phases of great differences play an important role.
2. Graphite phase is the microstructure that bears the highest conductivity among all microconstituents in cast irons. It also has an even greater anisotropic nature in comparison with pearlite structure. This causes a great effect on the effective thermal conductivity of different graphite morphology. More specifically, as high as 55 W/m/°C is achieved in cast irons with flake graphite, whereas only 25W/m/°C of thermal conductivity is obtained by nodular irons. The anisotropic effect is obvious. Furthermore, cast irons with compact graphite or the graphite with shapes in between flake and spheroids are shown to have thermal conductivity (~35 W/m/°C) more similar to the nodular irons rather than grey irons, even though the compact graphite shape appears closer to the flake graphite.
3. Effects of alloying elements on cast irons are also discussed by fixing the graphite as flake morphology. It is well known that the alloying elements pose both electron and phonon scattering effects in thermal conductivity. Meanwhile, there appears also great difference in the phase constituents due to alloying elements. Specifically, copper and aluminium additions promote graphite to form higher numbers of thinner graphite and reduce alloying reduction effects on thermal conductivity of cast irons. On the other hand, chromium and molybdenum additions cause the formation of carbides which not only increase thermal resistivity but also reduced graphite formation and therefore reduce thermal conductivity most severely among all alloying elements considered. It is thus concluded that the alloying elements affect thermal conductivity more by the amount of constituent phases rather than by the compositions of each phase.

4. Acknowledgment

The completion of this research is partly supported by the grant of National Science Council of Taiwan through #NSC98-2221-E-027-031 project. The materials supplied by China Metal Products and assistance of thermal conductivity measurements by EMO center at National Taipei University of Technology are acknowledged.

5. Appendix – list of symbols

A_i : phonon scattering due to impurity atoms, i .

C_i : concentration of i -th element in molar fraction

ε : thickness-length ratio of graphite

$f_{\text{Fe}_3\text{C}}$ and f_{ferrite} : volume fractions of Fe_3C and ferrite in pearlite, respectively

f_{other} volume fraction of other microconstituents such as austenite or carbides

$f_{\text{nodular graphite}}$ and $f_{\text{flake graphite}}$: fractions of graphite with nodular shape and flake shape, respectively.

$K_{e,\text{pure iron}}$: electron contribution in thermal conductivity of pure iron

$K_{e,\text{ferrite}}$: electron contribution in thermal conductivity of ferrite

$K_{p,\text{ferrite}}$: contribution of lattice vibration to thermal conductivity of ferrite

K_{ferrite} : thermal conductivity of ferrite

$K_{\text{Fe}_3\text{C}}$: thermal conductivity of cementite or 8 W/m/°C

$K_{\text{pearlite}}^{\text{eff}}$: effective isotropic thermal conductivity of pearlite

$K_{\text{pearlite},//}$ and $K_{\text{pearlite},\perp}$: thermal conductivity of pearlite in orientation parallel and perpendicular to the lamellae, respectively

$K_{\text{graphite},//}$ and $K_{\text{graphite},\perp}$: thermal conductivities of graphite in orientations parallel and perpendicular to the graphite surface, respectively

ρ_{m} : electrical resistivity of pure iron

K_{other} : thermal conductivity of other microconstituents such as austenite or carbides

L_e : Lorenze function relating $K_{e,\text{pure iron}}$ and ρ_{m} .

L_0 : the Sommerfeld-Lorenz number of $2.44 \times 10^{-8} \text{ W}\Omega^\circ\text{C}^{-2}$

ρ_i' : relative electrical resistivity of i -th alloying element in comparison with pure iron

$p_{//}$ and p_{\perp} : shape factors in orientations parallel and perpendicular to graphite flakes, respectively

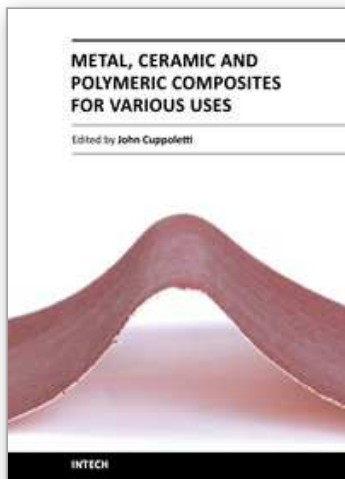
6. References

- Bruggeman, D.A.G. (1935). Dielectric constant and conductivity of mixtures of isotropic materials. *Ann. Phys. (Leipzig.)*, Vol.24, pp.636-679.
- Choy, T.C. (1999). *Effective Medium Theory, Principles and Applications*, Oxford Science Publications, ISBN 0198518927, New York, USA.
- Cheng, S.C. & Vachon, R.I. (1969). The prediction of the thermal conductivity of two and three phase solid heterogeneous mixtures, *Int. J. Heat Mass Transfer.*, Vol.12, pp.249-264.
- Gustafsson, S.E. (1991). Transient plane source techniques for thermal conductivity and thermal diffusivity measurements of solid materials, *Rev. Sci. Instrum.*, Vol.62, No.3, pp. 797-804.
- Helsing, J. & Grimvall, G. (1991). Thermal Conductivity of Cast Iron : Models and Analysis of Experiments. *Journal of Applied Physics*, Vol.70, No.3, pp.1198-1206.
- Helsing, J. & Helte. A. (1991) Effective conductivity of aggregates of anisotropic grains, *J. Appl. Phys.*, V.69, No.6, pp.3583-3588.
- Maxwell-Garnett, J.C. (1904). Colours in metal glasses and in metallic films. *Philos. Trans. R. Soc. A*, Vol.203, pp. 385-420.
- Schulgasser, K. (1977) Bounds on the conductivity of statistically isotropic polycrystals, *J. Phys. C: Solid State Phys.*, Vol.10, pp.407-417.

- Tsao, G.T.N. (1961). Thermal conductivity of two phase materials, *Ind. Engrg. Chem.*, Vol.53, No.5, pp.395-397.
- Williams, R.K. ; Yarbrough, D.W. ; Masey, J.W. ; Holder, T.K. & Graves, R.S. (1981). Experimental determination of the phonon and electron components of the thermal conductivity of bcc iron, *J. Appl. Phys.*, Vol.52, No.8, pp.5167-5175.

IntechOpen

IntechOpen



Metal, Ceramic and Polymeric Composites for Various Uses

Edited by Dr. John Cuppoletti

ISBN 978-953-307-353-8

Hard cover, 684 pages

Publisher InTech

Published online 20, July, 2011

Published in print edition July, 2011

Composite materials, often shortened to composites, are engineered or naturally occurring materials made from two or more constituent materials with significantly different physical or chemical properties which remain separate and distinct at the macroscopic or microscopic scale within the finished structure. The aim of this book is to provide comprehensive reference and text on composite materials and structures. This book will cover aspects of design, production, manufacturing, exploitation and maintenance of composite materials. The scope of the book covers scientific, technological and practical concepts concerning research, development and realization of composites.

How to reference

In order to correctly reference this scholarly work, feel free to copy and paste the following:

J.K. Chen and S.F. Chen (2011). Thermal Conductivity of an in-Situ Metal Matrix Composite - Cast Iron, Metal, Ceramic and Polymeric Composites for Various Uses, Dr. John Cuppoletti (Ed.), ISBN: 978-953-307-353-8, InTech, Available from: <http://www.intechopen.com/books/metal-ceramic-and-polymeric-composites-for-various-uses/thermal-conductivity-of-an-in-situ-metal-matrix-composite-cast-iron>

INTECH
open science | open minds

InTech Europe

University Campus STeP Ri
Slavka Krautzeka 83/A
51000 Rijeka, Croatia
Phone: +385 (51) 770 447
Fax: +385 (51) 686 166
www.intechopen.com

InTech China

Unit 405, Office Block, Hotel Equatorial Shanghai
No.65, Yan An Road (West), Shanghai, 200040, China
中国上海市延安西路65号上海国际贵都大饭店办公楼405单元
Phone: +86-21-62489820
Fax: +86-21-62489821

© 2011 The Author(s). Licensee IntechOpen. This chapter is distributed under the terms of the [Creative Commons Attribution-NonCommercial-ShareAlike-3.0 License](https://creativecommons.org/licenses/by-nc-sa/3.0/), which permits use, distribution and reproduction for non-commercial purposes, provided the original is properly cited and derivative works building on this content are distributed under the same license.

IntechOpen

IntechOpen